Article ID: 1006-8775(2019) 04-0528-14

PRELIMINARY STUDY ON THE INFLUENCE OF FY–4 LIGHTNING DATA ASSIMILATION ON PRECIPITATION PREDICTIONS

LIU Rui-xia (刘瑞霞)[1], LIU Jie (刘 杰)[2], PESSI Antti (帕茜·安蒂)[3], HUI Wen (惠 雯)[1], CHENG Wei (成 巍)[4], HUANG Fu-xiang (黄富祥)[1]

(1. Key Laboratory of Radiometric Calibration and Validation for Environmental Satellite/ National Satellite Meteorological Center, China Meteorological Administration, Beijing 100081 China; 2. China Meteorological Press, Beijing 100081 China; 3. Vaisala, Westford, MA 01886 USA; 4. Beijing Institute of Applied Meteorology, Beijing 100029 China)

Abstract: Data from the lightning mapping imager on board the Fengyun-4 meteorological satellite (FY-4) were used to study the assimilation of lightning data and its influence on precipitation predictions. We first conducted a quality control check on the events observed by the first Fengyun-4 satellite (FY-4A) lightning mapping imager, after which the noise points were removed from the lightning distribution. The subsequent distribution was more consistent with the spatial distribution and range of ground-based observations and precipitation. We selected the radar reflectivity, which was closely related to the lightning frequency, as the parameter to assimilate the lightning data and utilized a large sample of lightning frequency and radar reflectivity data from the eastern United States provided by Vaisala. Based on statistical analysis, we found the empirical relationship between the lightning frequency and radar reflectivity and established a look-up table between them. We converted the lightning event data into radar reflectivity data and found that the converted reflectivity and composite reflectivity of ground-based radar observations showed high consistency. We further assimilated the lightning data into the model, adjusted the model cloud analysis process and adjusted the model hydrometeor field by using the lightning data. A rainstorm weather process that occurred on August 8, 2017 in south China was used for the numerical forecast experiment, and three experiments were designed for comparison and analysis: a control experiment, an experiment without the assimilation of FY-4 lightning data (NoLig), and an experiment with the assimilation of FY-4 lightning data (Lig). The results show that after assimilating the FY-4A lightning data, the accuracies of the intensity, central location and range of the precipitation predicted by the Lig experiment were obviously superior to those predicted by the control and NoLig experiments, and the effect was especially obvious in the short-term (1–2 hour) forecast. The studies in this paper highlight the application value and potential of FY-4 lightning data in precipitation predictions.

Key words: FY-4 lightning data; data assimilation; cloud analysis; precipitation prediction

CLC number: P412.27 **Document code:** A

doi: 10.16555/j.1006-8775.2019.04.009

1 INTRODUCTION

In recent years, unconventional observation data obtained via satellite, radar, global positioning systems (GPSs), and microwave radiometers, etc., have been successfully applied to the assimilation of initial fields in numerical models, and they have greatly improved the accuracy of numerical model precipitation predictions (Liu et al.[1]; Zhao and Liu [2]). In conjunction with the rapid development of lightning detection techniques and research on the relationships between lightning observation data and precipitation and between lightning observation data and strong convective systems, the assimilation of lightning data and the applications of numerical weather forecast have become important research subjects (Liu et al. [3]). Nevertheless, the assimilation of lightning data is difficult to perform because lightning events, lightning frequencies, electric field distributions and electric charge densities are not the modeled variables or diagnostic quantities of numerical models. Therefore, appropriate observation operators must be identified to connect lightning observation variables with model variables or diagnostic variables; alternatively, a proxy variable of lightning data with strong physical meaning must be established to achieve the assimilation of lightning data. Over the past decade, many researchers have investigated the microphysical mechanisms of convective clouds to identify reliable associations between lightning data and other meteorological variables, and a number of methods have been employed to assimilate lightning data, which has yielded valuable results. Chang et al. and Pessi and

Received 2019-01-09; **Revised** 2019-08-06; **Accepted** 2019-11-15

Foundation item: National Key Research and Development Program of China (2018YFC1506603, 2016YFB0502501); National Natural Science Foundation of China (41505028, 41705033)

Biography: LIU Rui-xia, Ph. D., primarily undertaking research on satellite data assimilation and weather forecast.

Corresponding author: LIU Jie, e-mail: rajliuj@163.com

Businger established the relationship between lightning and convective precipitation and showed that the assimilation of lightning data increased the accuracy of winter storm simulations over the North Pacific Ocean [4, 5]. Wang et al. concluded that the precipitation process, especially the storm center and its intensity, can be better simulated through the assimilation of lightning flashes by utilizing the statistical relationship between lighting activity and convective precipitation[6]. The United States' operational Rapid Update Cycle (RUC) assimilation system, which was replaced by the Rapid Refresh (RAP) system in 2012, converts lightning data into three-dimensional proxy radar echo intensities in its cloud analysis module and further adjusts the microphysical quantities and water vapor in the cloud. Moreover, the RUC system calculates the temperature tendency, which is used to replace the temperature tendency generated by the microphysical process of the model and the convection parameterization scheme in the forward integral process of the diabatic digital filter initialization (DDFI) model, and the parameterization scheme that inhibits cumulus convection in locations without a composite echo plays a very important role in the near-shore forecast (Benjamin [7]). Fierro et al. established an empirical relationship among the water-vapor mixing ratio, lightning frequency and graupel mixing ratio in the Weather Research and Forecasting (WRF) model and obtained a more accurate simulation for the tornado that occurred on May 24, 2011, in Oklahoma of the United States [8]. Qie et al. established an empirical relationship between lightning frequency and ice-phase particle content and used SAFIR (Surveillance et Alerte Foudre par Interfé rometrie Radioé lectrique) total lightning data to adjust the content of ice-phase particles (ice, snow and graupel) in the WRF single-moment 6-class (WSM6) microphysical scheme. The experimental results indicate that this method can improve the short-term precipitation prediction of mesoscale convective systems (MCSs) [9]. Marchand and Fuelberg developed a new method that heats the most unstable layer at the position of convection indicated by lightning and further improved the initialization of convection in the model. They found that this method is more effective for isolated thunderstorm cells or thunderstorm weather processes subject to the small influences of a weather system [10]. Stefanescu et al. converted lightning data into proxy convective available potential energy (CAPE) and adopted the variational method to assimilate lightning data from the Earth Networks Total Lightning Network (ENTLN) and to analyze two strong convection processes. The results showed that this scheme can effectively reduce the root-mean-square error of precipitation predictions [11]. Mansell et al. established a linear statistical relationship between the lightning frequency and hail and graupel echoes as the observation operator and applied the ensemble Kalman filter (EnKF) method to assimilate the total lightning data, the results of which indicated an obvious improvement [12].

Lightning data have numerous advantages; for example, they boast a wide observation range, reliable quality and high spatial resolution, and they are not restricted by mountains or oceans. Thus, these data have received increasing attention for research purposes. The lightning observation data used within the international community are obtained primarily from ground-based lightning observation networks and low-Earth orbit satellites, which unfortunately suffer from a limited detection range and cannot comprehensively monitor, track or provide early warning of lightning in the same region in real time. The first Fengyun-4 satellite (FY-4A) of China was successfully launched in December 2016. The onboard lightning mapping imager (LMI) was the first optical load sensor for lightning detection in geostationary orbit developed by China (Liang et al.[13]). This imager was developed during the same period as the other two optical lightning detection loads in geostationary orbit launched by the United States and Europe. Optical lightning detection sensors in geostationary orbit adopt the gazing manner to achieve the continuous and real-time detection of lightning in the same region; this approach constitutes one of the most effective methods of lightning detection (Christian et al. [14]). Although the field of view covers all of China and its surrounding areas, the other indexes of the FY-4A LMI are essentially consistent with the Lightning Imager (LI) of the European Meteosat Third Generation (MTG) and the Geostationary Lightning Mapper (GLM) of the United States' Geostationary Operational Environmental Satellite (GOES)-R series (Finke [15]; Bao et al.[16]). The GOES-R platform was launched in November 2016, and the MTG satellite is scheduled to launch in 2020. The assimilation of FY-4A lightning data has important potential for applications in operational numerical weather prediction. Therefore, in this paper, valuable FY-4A lightning observation data are used to assimilate lightning data and evaluate the influences of these data on precipitation predictions.

2 DATA DESCRIPTION

In this paper, we select Level-1B (L1B) data obtained by the FY-4A LMI, namely, the event data of LMI observations. Events are the most basic form of lightning detection data obtained by the LMI. Clustering calculations and treatments are performed to generate lightning imaging products on different levels of the event-group-flash. The FY-4A LMI continuously detects lightning at 2 m s^{-1} intervals. The lightning event data are stored each minute as one packet in an HDF format. The data used in this paper are processed through the preliminary filtering of false signals (Hui et al. [17]).

3 SELECTION OF CASES

We adopted the rainstorm that occurred in south China during August 8 – 9, 2017, to conduct the

experiment. During this event, heavy rain and torrential rain fell over the middle and lower reaches of the Yangtze river, and Yunnan and Guizhou provinces of China. Fig. 1 shows the distribution of the 24-hour precipitation from 0 (UTC) on August 8, 2017, to 0 (UTC) on August 9, 2017, and the 500-hPa circulation pattern at 0 (UTC) on August 8, 2017. The precipitation data are from ground-based precipitation gauge observations, and the 500-hPa circulation data are from the National Centers for Environmental Protection (NCEP) final analysis (FNL) data. The middle and lower reaches of the Yangtze River region was dominated by short-term strong precipitation, and some areas experienced thunderstorms and strong winds. In particular, the hourly precipitation in northern Hunan and local regions of Jiangsu exceeded 130 mm (Fig. 1a). This precipitation event was affected mainly by a high-level trough and low-level shear. The high-level circulation pattern (Fig. 1b) shows that a high-level trough at 500 hPa moved eastward and southward. Precipitation-producing clouds appeared over the area of the middle and lower reaches of the Yangtze River, northern Hunan and the Yunnan-Guizhou area.

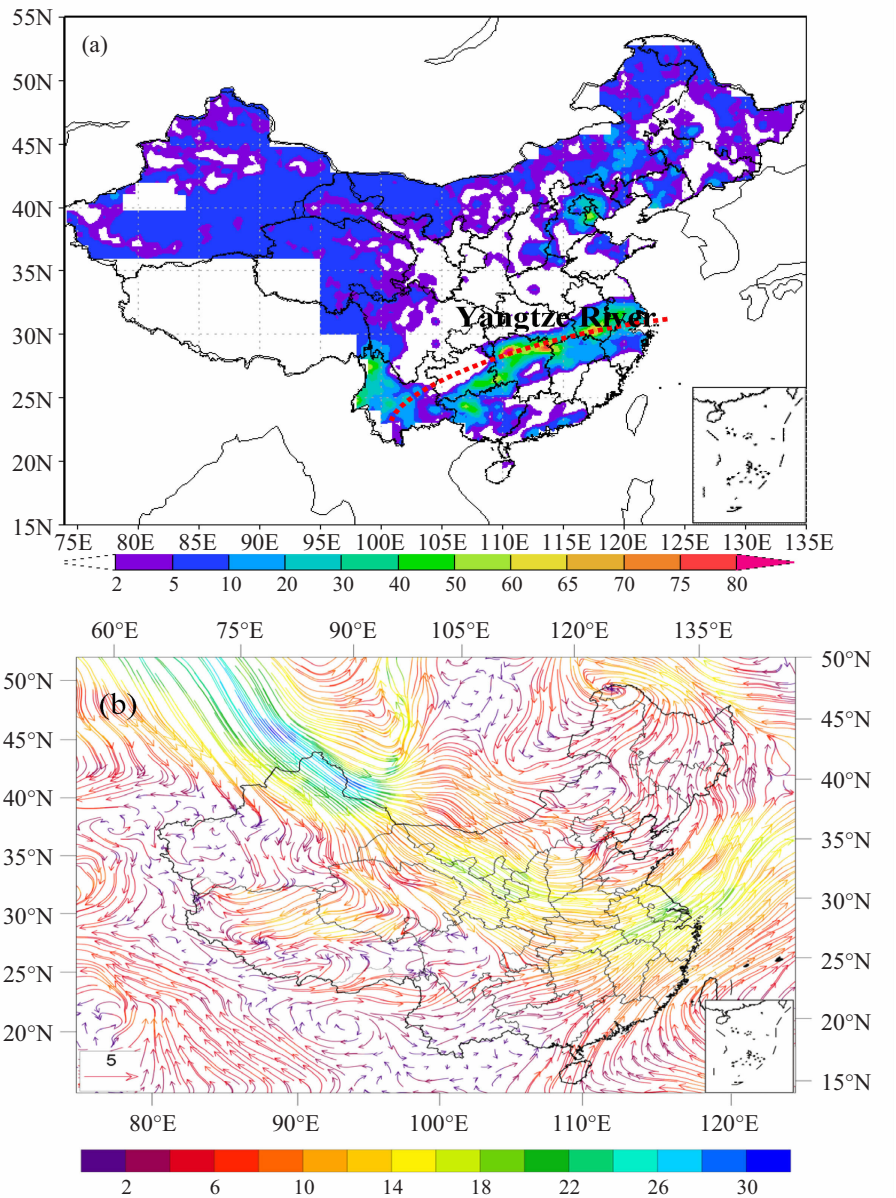

Figure 1. (a) Distribution of the 24-hour precipitation from 12 (UTC) on August 8, 2017, to 11 (UTC) on August 9, 2017, and (b) the 500-hPa circulation pattern at 11 (UTC) on August 8, 2017.

4 MODEL AND EXPERIMENTAL DESIGN

The Local Analysis and Prediction System (LAPS) developed by the Earth System Research Laboratory (ESRL) in affiliation with the National Oceanic and Atmospheric Administration (NOAA) of the United States was used for the lightning data assimilation in this paper. LAPS is an integrated system that ingests and analyzes meteorological data from different observational

sources. This system can combine and harmonize input data (such as data from meteorological ground observation networks, radars, satellites, sounding detectors, and airplanes) to derive surface and 3D fields of the temperature, geopotential or pressure, humidity, wind and cloud parameters with a high resolution. In our study, the LAPS cloud analysis was adjusted to generate the initial field of the prediction model.

WRF3.4 was adopted as the forecast model. The WRF model was designed for both atmospheric research and operational forecasting applications as a result of a collaborative partnership among the National Center for Atmospheric Research (NCAR), NOAA, NCEP and other companies and universities. This forecast model has been widely used around the world due to its state-of-the-art science, flexibility and ease of use.

In this study, the assessed domain spans the quadrant bounded by 21°N–34°N, 99°E–122°E, and the center of the simulated area is located at 110°E, 28°N. We used 27 terrain-following (eta) levels in the vertical direction. The grid size is 5 km; without nesting, the grid includes 451 points in the east-west direction and 281 points in the north-south direction. The parameterization schemes of physical processes employed within the WRF model in this study (Table 1) include mainly the WRF single-moment 3-class (WSM3) physical scheme, the Kain-Fritsch cumulus convection scheme, the rapid radiative transfer model (RRTM), the Dudhia shortwave radiation scheme, the Yonsei University (YSU) boundary layer process scheme, and the 5-layer thermal diffusion land surface parameterization scheme.

The NCEP Global Forecast System (GFS) product is used for the initial field and boundary conditions. The starting forecast time is 11 (UTC) on August 8, 2017, and the forecast period is 24 hours.

Table 1. Parameterization schemes of physical processes within the WRF model.

Classification of schemes	Scheme option
Domain design	451*281 grids, resolution: 5 km
Physical parameterization scheme	WRF single-moment 3-class (WSM3) scheme
Longwave radiation scheme	Rapid radiative transfer model (RRTM)
Shortwave radiation scheme	Dudhia shortwave radiation scheme
Cumulus parameterization scheme	Kain-Fritsch scheme
Boundary layer process scheme	Yongsei University (YSU) scheme
Land surface process scheme	5-layer thermal diffusion land surface scheme

Three experiments were designed in this paper to compare the effects of assimilating FY-4 lightning data. The experiments are described in Table 2.

(1) Comparison Experiment 1 (denoted as Control). No real observations were assimilated.

(2) Comparison Experiment 2 (named as NoLig). The initial fields of the forecast model were provided by LAPS, and the FY-4 lightning data were not assimilated.

(3) Comparison Experiment 3 (hereafter referred to as Lig). The only difference between this experiment and the NoLig experiment is that FY-4 lightning data were assimilated while the initial fields were generated.

The period in which the occurrence of lightning was relatively concentrated starting at 11 (UTC) on August 8, 2017, was selected, and the lightning data were assimilated at 11 (UTC). We conducted three prediction experiments and compared the results with the actual precipitation conditions for evaluation.

Table 2. Experimental schemes and assimilation data.

Name of experiment	Data assimilation
Control	No data assimilation and cold start. No hydrometeor was used in the initial field.
NoLig	No assimilation of FY-4 lightning data. The LAPS hydrometeor output was used as the initial field of the model to hot start the model.
Lig	FY-4 lightning data were assimilated, and the LAPS hydrometeor output was used as the initial field of the model to hot start the model.

5 QUALITY CONTROL OF THE FY – 4 LIGHTNING DATA

Before assimilating the lightning data, a quality control check, which represents a critical step, was performed. Fig. 3 shows the distribution of FY-4 lightning at the assimilation time. Although the selected lightning event data were preliminarily processed by filtering out noise, a large amount of noisy points remained.

Therefore, quality control was further performed on the FY-4 lightning events within the observation data.

During the quality control process, a threshold is set, and the lightning data are filtered such that only those within 10 minutes before and after the assimilation time remain. For every observation point, if the number of lightning events within 10 minutes before and after the assimilation time exceeds the threshold, the lightning observation at this point is considered effective and is included in the assimilation. Fig. 2 shows the distribution of lightning events before and after the quality control process. Fig. 2a shows a map of the lightning distribution at the assimilation time, i.e., 11 (UTC) on August 8, 2017 before performing quality control, Fig. 2b shows a map of the cumulative lightning distribution within 10 minutes before and after the assimilation time after performing quality control, and Fig. 2c shows the lightning distribution ascertained by ground-based observations within 10 minutes before and after the corresponding assimilation time.

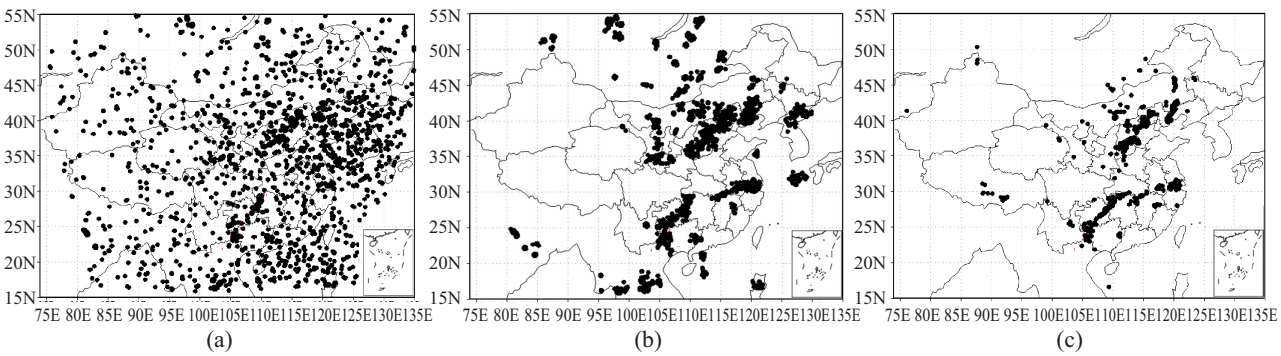

Figure 2. Distribution of FY-4A lightning events (a) before quality control and (b) after quality control; (c) lightning distribution determined from ground-based observations.

Compared with the ground-based lightning distribution (Fig. 2c), many sporadic points were effectively filtered out of the lightning distribution after performing quality control, and the distribution of lightning was more consistent with that determined from the ground-based observations. The cumulative number of lightning events in the research area within 10 minutes before and after 11 (UTC) is shown in Fig. 3. Lightning occurred mainly in the central region consisting of Guizhou, Hunan and Anhui, and the number of lightning strikes in this central region reached 1,549. Therefore, at the assimilation time, the convective activity in the precipitation region was strong, and lightning activity was frequent.

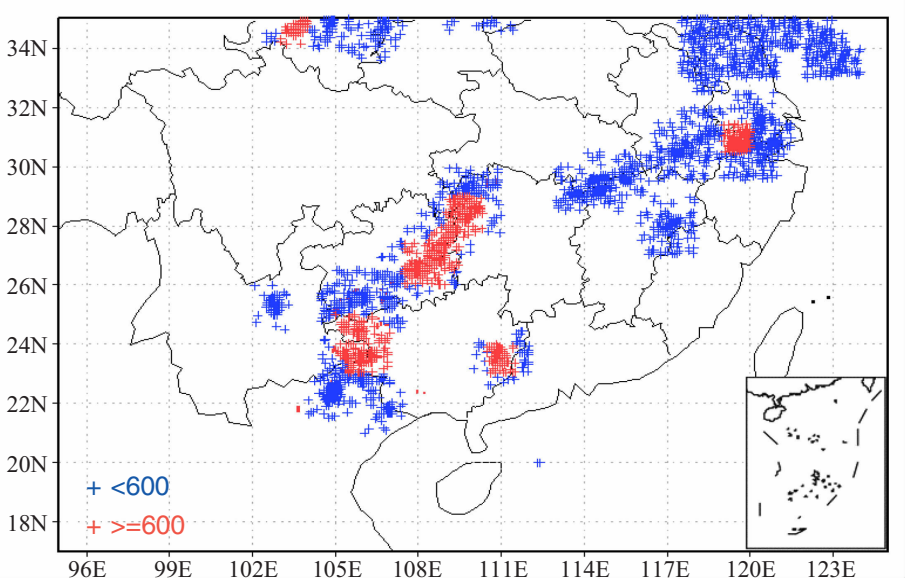

Figure 3. Cumulative number of lightning events within 10 minutes before and after 11 (UTC) on August 8, 2017.

6 ASSIMILATION METHOD

Establishing a relationship between the lightning frequency and the model variables is the key to lightning data assimilation. In this paper, we select radar reflectivity, which demonstrates a close relationship with lightning activity, as the parameter to assimilate lightning data. By using a large sample of lightning frequency and radar reflectivity data, we statistically obtained an empirical relationship between lightning frequency and

radar reflectivity. The sample lightning and radar reflectivity data were provided by Vaisala Inc. The data include a total of 226,000 samples over five months from the northeastern region of the United States as well as a large data sample over the oceans and continents (Pessi[18]; Pessi and Albers [19]). The lightning data were obtained from Vaisala's National Lightning Detection Network (NLDN) and Global Lightning Dataset (GLD360), and the radar data were acquired from the National Weather Service Next-Generation Weather Radar (NEXRAD). Preliminary results showed a strong lognormal correlation between the lightning frequency and radar reflectivity (Pessi [18]; Said and Inan [20]). Therefore, the collected lightning rates were divided into binned categories using an exponential division scheme (i.e., $2^n...2^{n+1}$), resulting in 8 different lightning categories for the NEXRAD-NLDN dataset (Pessi [18]). For each of these 8 categories, the average radar reflectivity profile was calculated (Fig. 4). Under each of the 8 lightning frequency categories, the radar reflectivity decreases as the height increases.

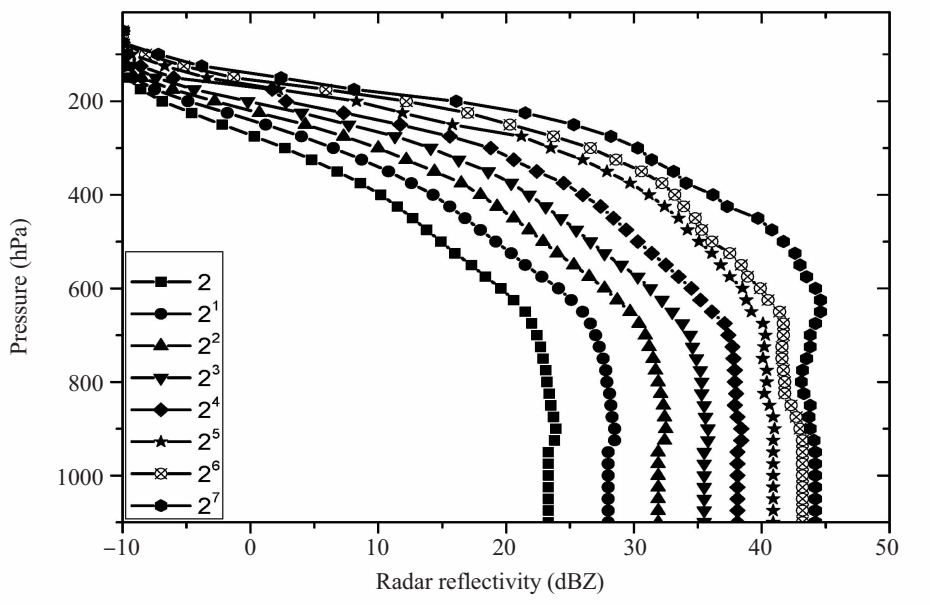

Figure 4. Statistical relationship between the lightning frequency and radar reflectivity.

Based on the above relationship, we converted the FY-4 lightning data observed at 11 (UTC) on August 8, 2017, into the radar reflectivity, as shown in Fig. 5a. The composite reflectivity of the actual radar observations is shown in Fig. 5b. A comparison analysis reveals that the proxy radar reflectivity obtained via the conversion of FY-4 lightning data was consistent with the actual ground-based radar observations regarding both the spatial distribution and the order of magnitude. Therefore, FY-4 lightning data can capture the strong signal of heavy precipitation and can thus be used for precipitation predictions.

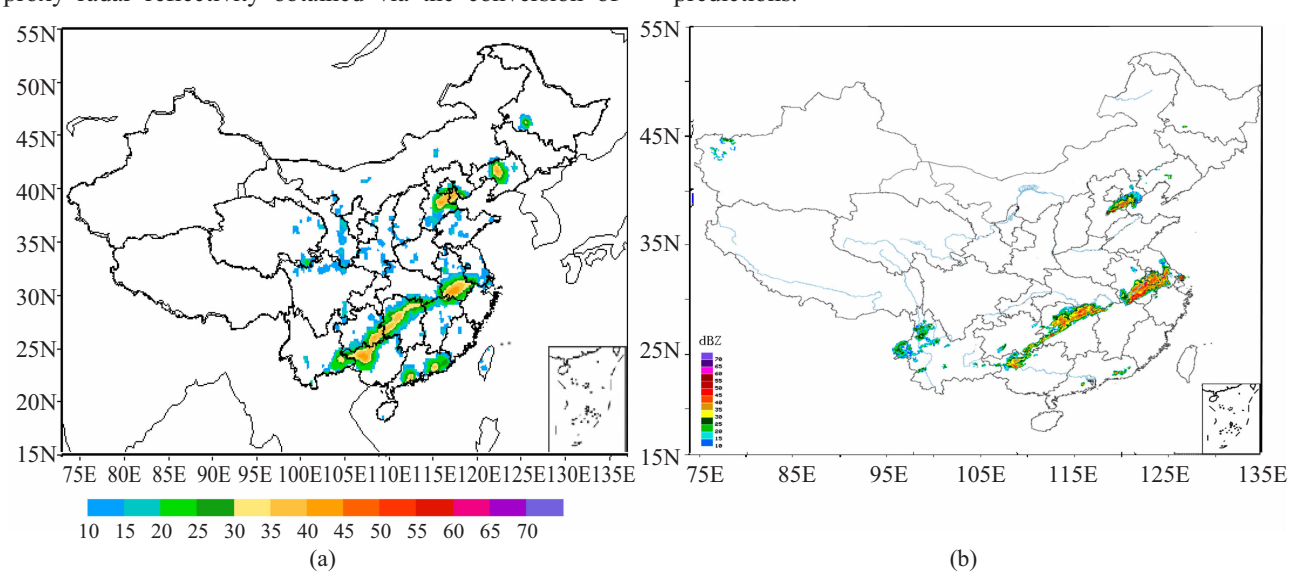

Figure 5. (a) Radar reflectivity at 11 (UTC) on August 8, 2017, converted from FY-4 lightning events and (b) ground-based composite radar reflectivity.

7 ANALYSIS OF THE INFLUENCE OF FY-4 LIGHTNING DATA ASSIMILATION ON PRECIPITATION PREDICTIONS

7.1 *Comparison and analysis of the initial field*

In this paper, we converted the observation data of FY-4 lightning events into radar reflectivity, which was assimilated into the model, and we adjusted the model's hydrometeor field using lightning data, which further affected the initial field of the forecast model. The hydrometeors obtained by the LAPS simulation included mainly the cloud water content, cloud ice content, rainwater content and snow particle content. Fig. 6 shows the hydrometeor distribution before (Fig. 6b) and after (Fig. 6a) the assimilation of the FY-4 lightning data. For the sake of brevity, we present only the distribution at 500 hPa, while the distributions for other layers are not shown. Before the assimilation of lightning data, the hydrometeor distribution in the research region was relatively uniform, and the hydrometeor content was essentially less than 0.0001 g kg $^{-1}$. The hydrometeor content in the relatively high-value region of southwestern Hubei was also less than 0.0004 g kg $^{-1}$. After assimilating the lightning data, the hydrometeor distribution range was relatively expanded within the precipitation zone. In addition, large-value hydrometeor regions were observed over Hunan, Guizhou, Yunnan, Guangxi, Anhui and Zhejiang, and the values exceeded 0.001 g kg $^{-1}$. The distribution of large-value regions consistently corresponded with the lightning frequency and the high-value regions of radar echoes obtained through the abovementioned conversion. Therefore, after assimilating the lightning data, the convective triggering in the corresponding high-precipitation regions was intensified; the hydrometeor particles appeared in these clouds were necessary carriers for the charge associated with the electrification process.

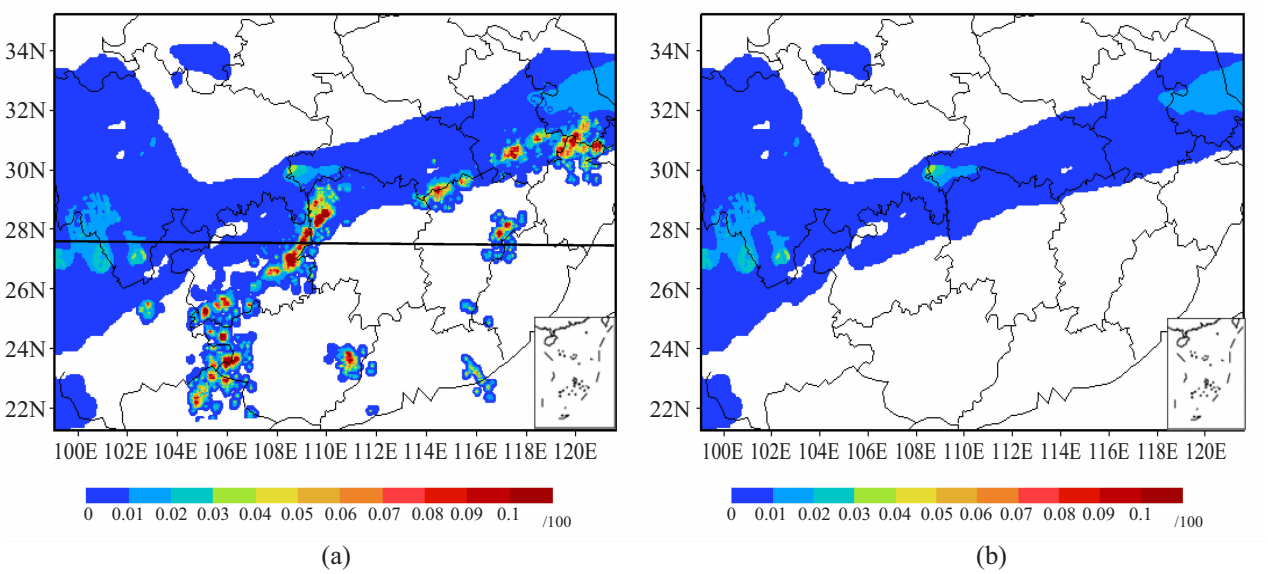

Figure 6. Distribution of the cloud hydrometeor in the two assimilation experiments at 500 hPa: (a) Lig experiment; (b) NoLig experiment (unit: g kg^{-1}).

Figures 7–10 show profiles of the cloud water content, cloud ice content, rain water content and snow particle content along 27.8°N. Fig. 6a shows the location of the profile line. A comparison of the results from the two experiments (Lig and NoLig) shows that after assimilating the lightning data, the hydrometeor content increased sharply. Near 110° E and 117° E along the profile, the amount of liquid water in the clouds increased, and the cloud water content increased from 0 to a high value of 0.004 g kg^{-1} (Fig. 7a). The ice water content (Fig. 8a), rainwater content (Fig. 9a) and snow particle content (Fig. 10a) at the corresponding locations increased, and the cloud top rose (Fig. 8a). The height of the cloud top without assimilating lightning data was approximately 250 hPa, whereas that after assimilating the lightning data extended to approximately 50 hPa, indicating that convective triggering at the location corresponding to frequent lightning was strengthened and that cloud formation was more vigorous after assimilating the lightning data.

7.2 *Influence of FY-4 lightning data assimilation on precipitation predictions*

We conducted a 24-hour precipitation forecast experiment and compared and analyzed the hourly precipitation results simulated in the three forecast experiments. Fig. 11 shows the results of 1-hour precipitation predictions for the three experiments and the actual precipitation distribution. The actual precipitation conditions indicate that precipitation was concentrated mainly north of Zhejiang, south of Anhui, at the

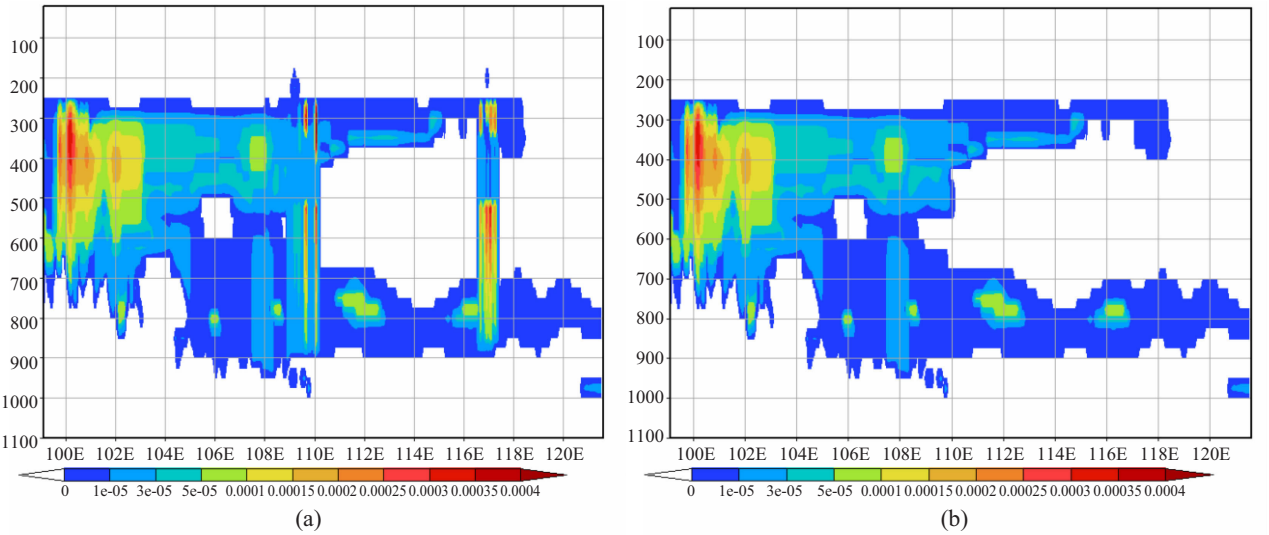

Figure 7. Profile of the cloud water content along 27.8° N in the two assimilation experiments: (a) Lig experiment; (b) NoLig experiment (unit: g kg^{-1}).

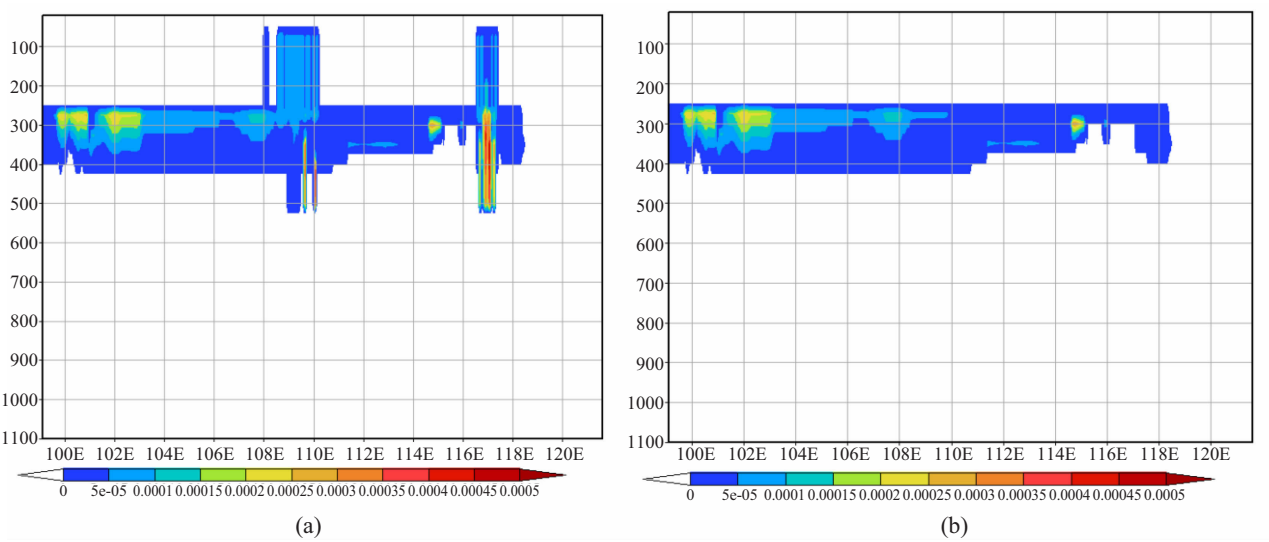

Figure 8. Profile of the cloud ice content along 27.8°N in the two assimilation experiments: (a) Lig experiment; (b) NoLig experiment (unit: g kg^{-1}).

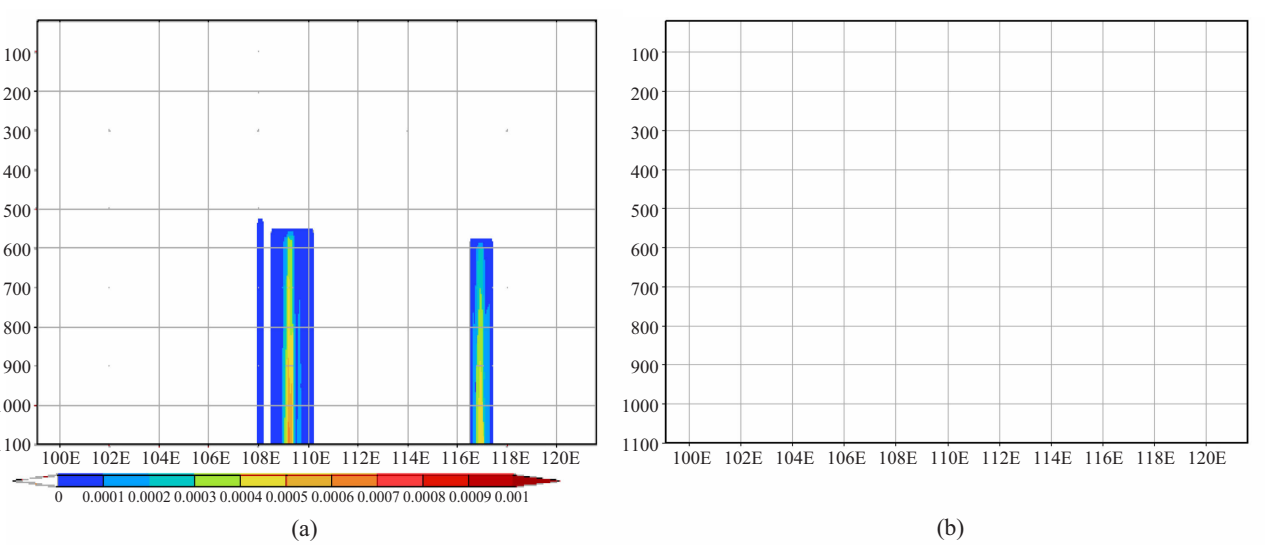

Figure 9. Profile of the rainwater content along 27.8°N in the two assimilation experiments: (a) Lig experiment; (b) NoLig experiment (unit: g kg^{-1}).

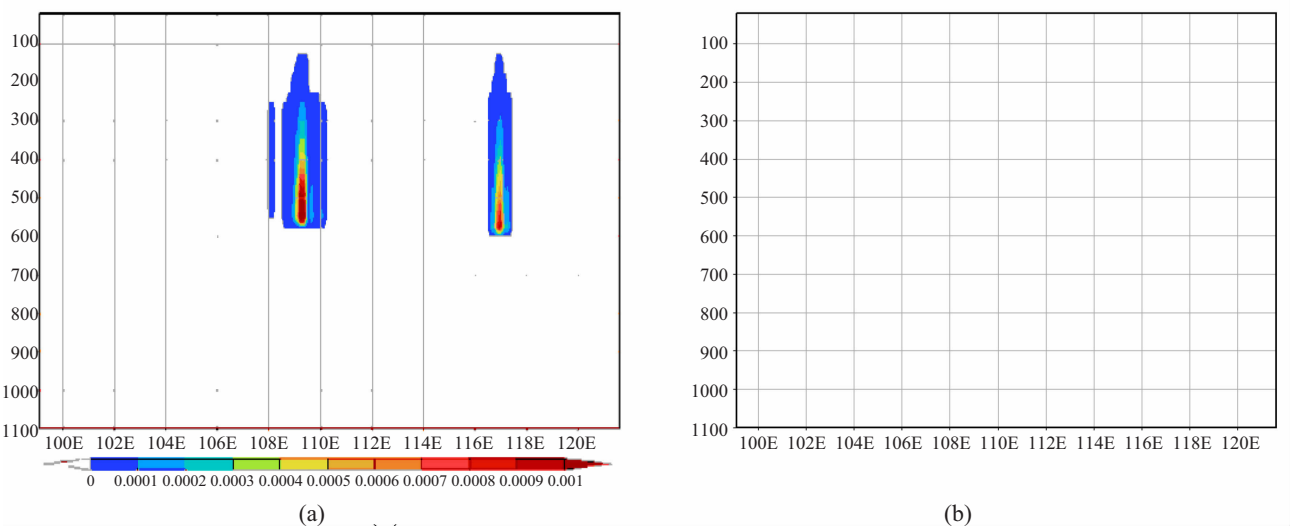

Figure 10. Profile of the snow particle content along 27.8°N in the two assimilation experiments: (a) Lig experiment; (b) NoLig experiment (unit: g kg^{-1}).

Hubei-Jiangxi junction, north of Hunan and in central Guizhou, and obvious characteristics of convective precipitation were observed. The precipitation zone exhibited a zonal distribution pattern from southwest to northeast. The precipitation center was over Zhejiang, south of Hubei and north of Hunan, and the maximum hourly precipitation reached 62 mm (Fig. 11d). The precipitation range predicted by the control experiment was obviously smaller than the actual range because it simulated only the sporadic precipitation zones in the range of the precipitation zone, and the order of magnitude was also obviously smaller than the actual magnitude because of the spin-up problem observed during the model's initial prediction (Fig. 11a). In the NoLig experiment, the cloud and rain information of the LAPS analysis was input into the initial field; therefore, the predicted outcome was better than that of the control experiment. Precipitation was predicted south of Anhui, north of Hunan and over central Guizhou, although the range and magnitude of the precipitation zone deviated considerably from the actual situation. Moreover, the large-range precipitation zones over the Hubei-Jiangxi junction and Guizhou were missing (Fig. 11b). After assimilating the lightning data (Fig. 11c), the precipitation zone of the assimilation experiment from southern Anhui to central Guizhou was much closer to the actual situation compared with those of the control experiment and NoLig experiment, although the amount of precipitation simulated for the area north of Zhejiang was smaller than the actual amount. The precipitation zone over the area north of Zhejiang also corresponded to the poorest predicted outcome among the three experiments.

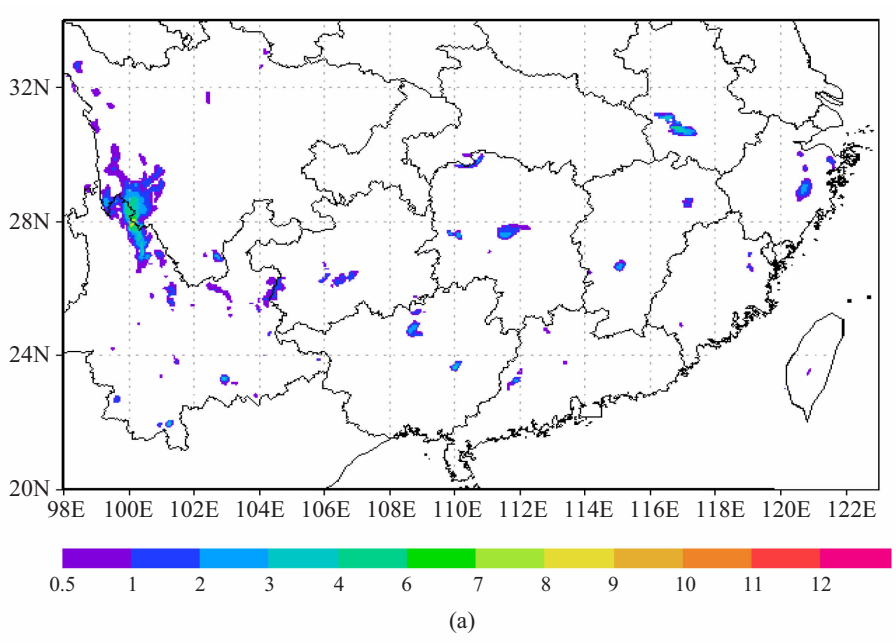

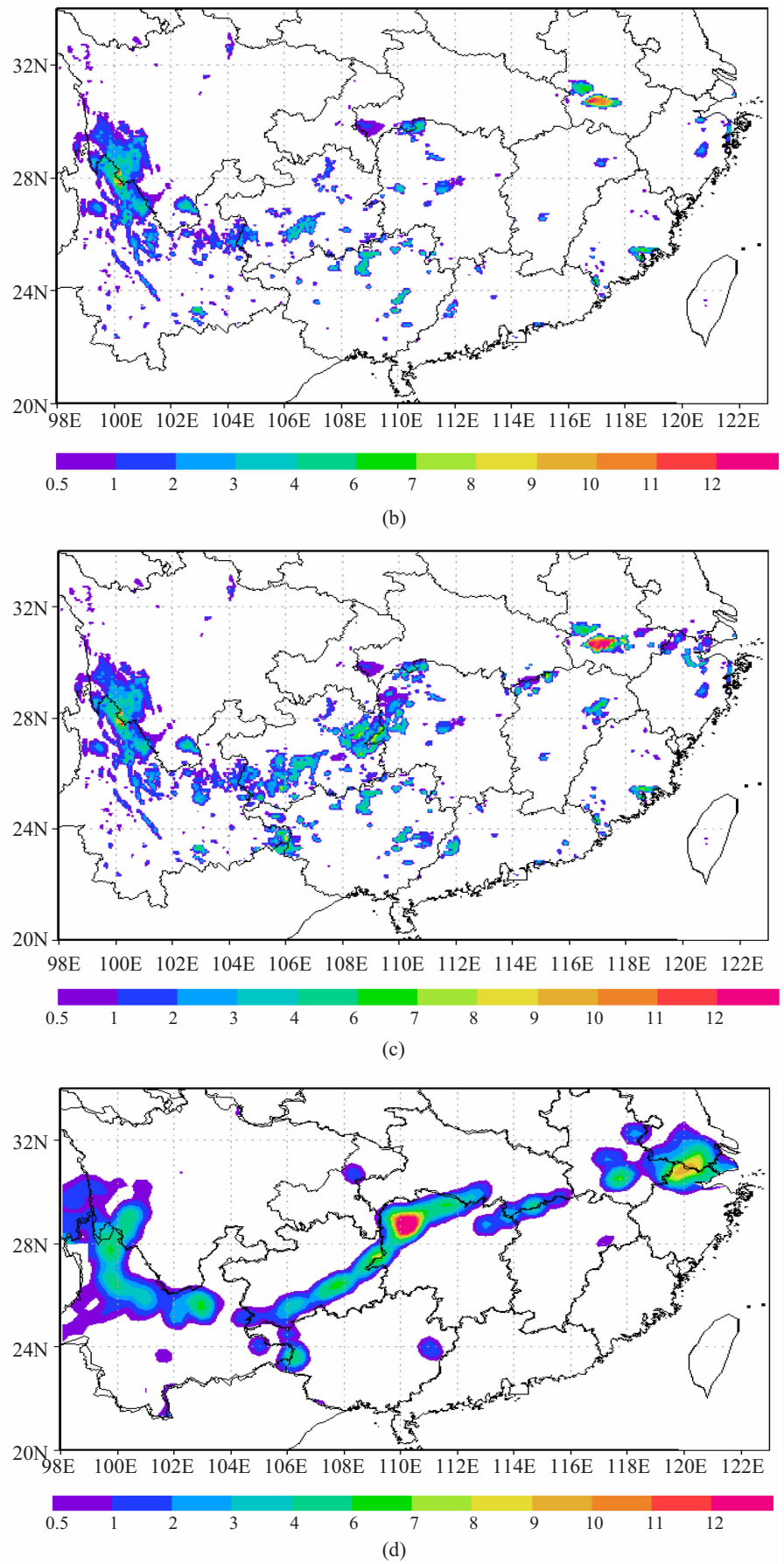

Figure 11. The 1-hour accumulated rainfall distribution from 12 (UTC) to 12 (UTC) on August 8, 2017, and the real observations: (a) control experiment; (b) NoLig experiment; (c) Lig experiment; and (d) actual precipitation from ground observations.

After 2 hours, the range and position of the precipitation area based on the actual situation were stable and did not show considerable movement, and the amount of precipitation at the center increased (not shown). The precipitation center and precipitation amount predicted by the control experiment were still smaller than the actual values, although this experiment predicted the precipitation center over southern Anhui. The NoLig experiment predicted the precipitation region over Guizhou, although the order of magnitude was slightly smaller than the actual situation. Compared with the first two experiments, after assimilating the lightning data, the precipitation range and order of magnitude for the precipitation area of the Lig experiment were still the best among the three experiments.

Fig. 12 shows the cumulative precipitation distribution of the 6-hour forecast. According to the results of the 3- to 6-hour forecast experiments, the control experiment still presented the spin-up phenomenon, and the predicted precipitation range was smaller than the actual situation. However, as the integration time of the model increased, the model integrated the cloud and rain information, and the predicted amount of precipitation increased. The precipitation range predicted by the NoLig experiment was also closer to the actual situation, and the relative performance of the Lig experiment was better. For the model integration time of 24 hours, the precipitation range and order of magnitude predicted by the NoLig experiment were essentially consistent with those predicted by the Lig experiment, and the precipitation predicted by the control experiment over the Hubei-Jiangxi junction was still smaller than the actual precipitation (Fig. 13).

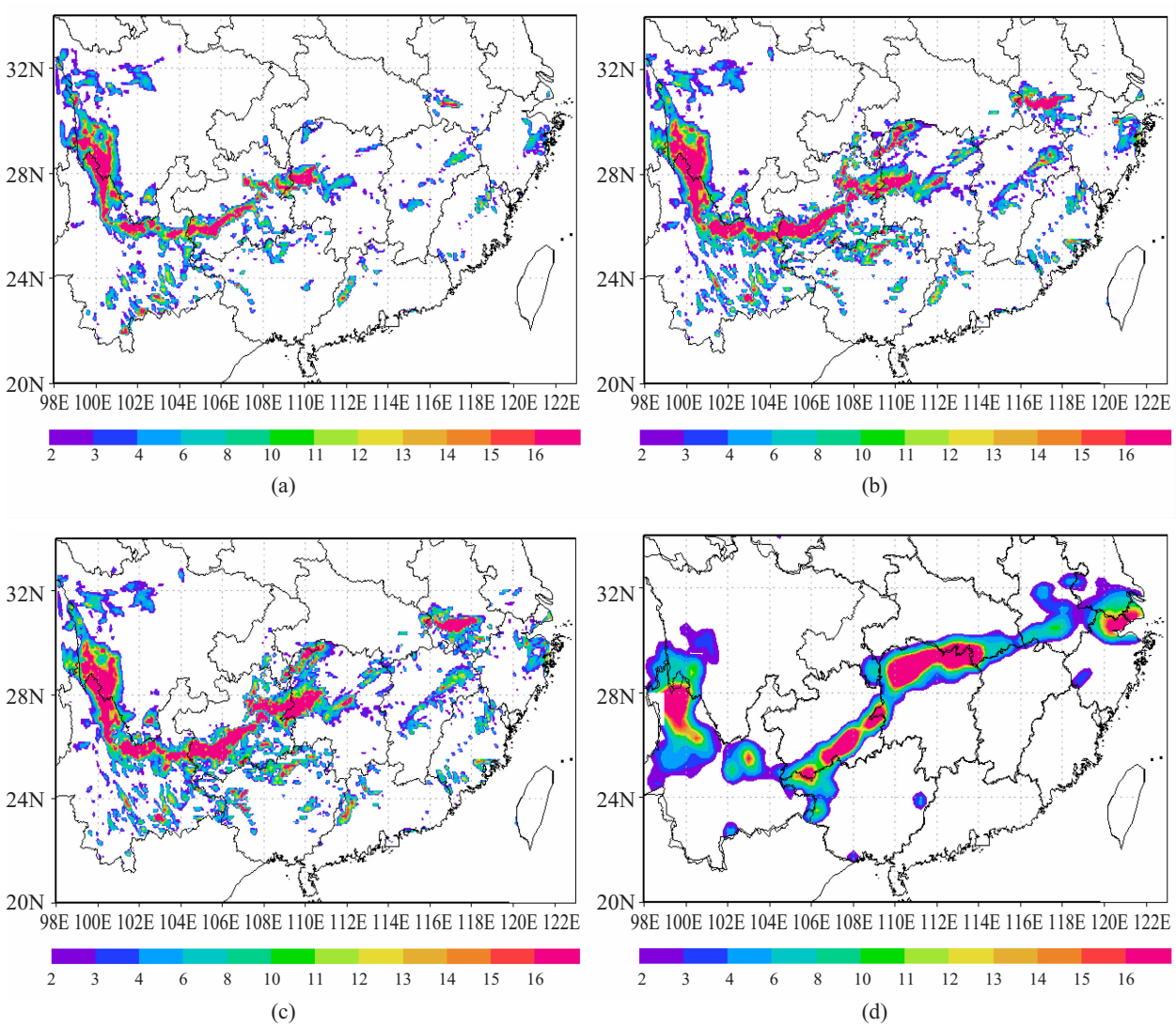

Figure 12. The 6-hour accumulated rainfall distribution from 12 (UTC) to 17 (UTC) on August 8, 2017, and the real observations: (a) control experiment; (b) NoLig experiment; (c) Lig experiment; and (d) actual precipitation of ground observations.

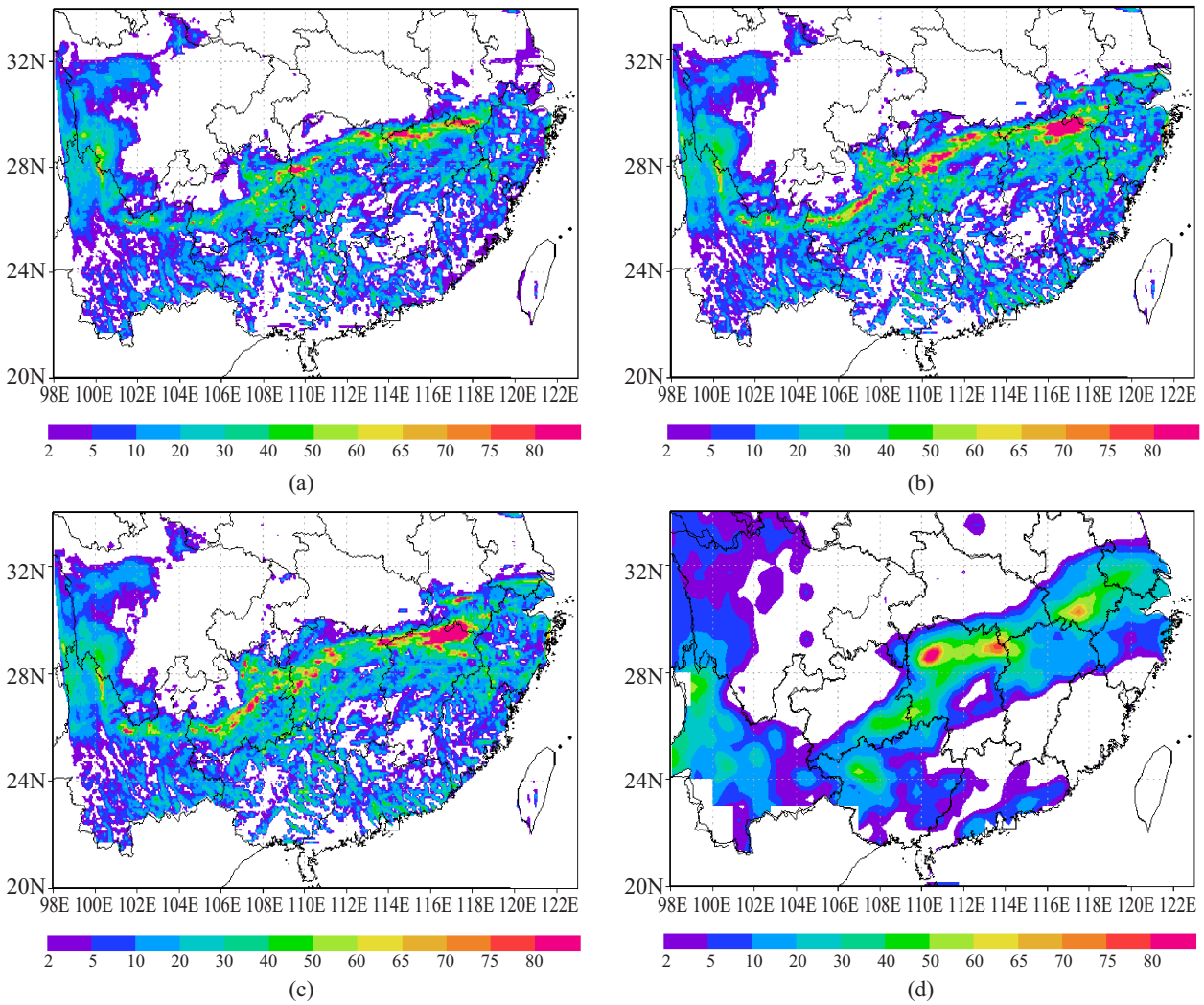

Figure 13. The 24-hour accumulated rainfall distribution from 12 (UTC) on August 8, 2017, to 11 (UTC) on August 9, 2017, and the real observations: (a) Control experiment; (b) NoLig experiment; (c) Lig experiment; and (d) actual precipitation of ground observations.

A comprehensive comparison shows that differences occurred in the amount of precipitation predicted within 1–24 hours by the different schemes, although the greatest differences were observed mainly in the first 6 hours. At subsequent integration times, although the amount of precipitation predicted by the different schemes differed in quantity, the differences were very small. Therefore, after the FY-4A LMI lightning observation data were assimilated into the initial field of the model, the initial cloud and hydrometeor model fields were improved, thereby improving the local strong precipitation forecasts. In summary, the assimilation of lightning data effectively improved the 1–6 hour forecast results for the extent and intensity of precipitation.

For the precipitation predictions, the threat score (TS), probability of detection (POD), equitable threat score (ETS) index and bias (BIAS) were determined. The TS indicates the forecast accuracy and reflects the degree of accuracy for an effective precipitation prediction; the ideal value is 1. The POD reflects the accuracy and indicates that the frequency of precipitation is also contained within the meteorological observations when a precipitation event is observed; therefore, the POD indicates whether the model can identify precipitation, and the ideal value is 1. The ETS index considers the randomness of precipitation, and it is often used to compare the accuracy of precipitation predictions between different regions or on different timescales. The BIAS value of a precipitation prediction reflects the ratio between the number of grid points with predicted precipitation and the number of grid points with an actual precipitation event in the statistical region. Therefore, a BIAS value closer to 1 indicates that the prediction range is closer to the actual situation, while BIAS>1 indicates that the prediction range is larger than the actual range, and BIAS<1 indicates that the prediction range is smaller than the actual range.

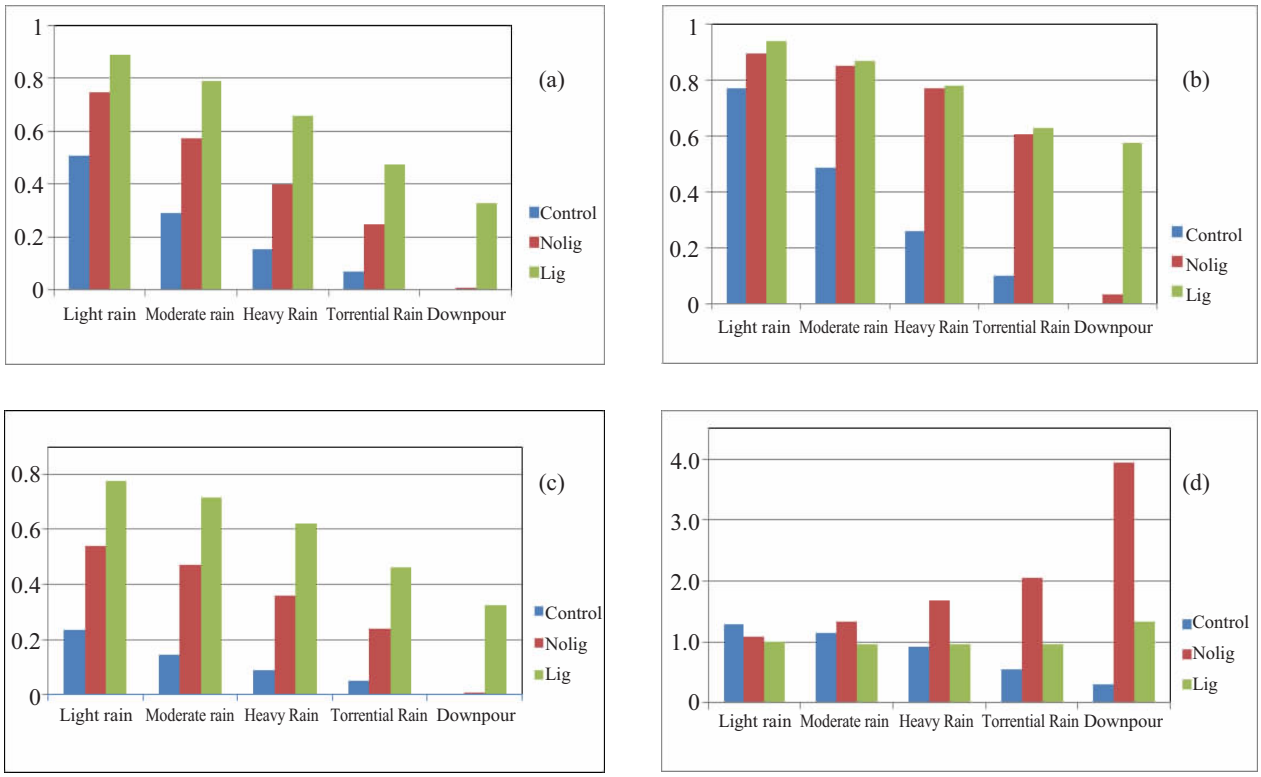

Figure 14. The (a) TS, (b) POD, (c) ETS and (d) BIAS of the 24-hour precipitation forecast for the three experiments.

Figure 14 shows the TS, POD, ETS and BIAS values for the three experiments. After assimilating the FY-4 lightning data (Green column), the TS and ETS values of the 24-hour precipitation forecast of the Lig experiment were both higher than those of the other two experiments. The accuracy increased, and the deviation decreased.

8 CONCLUSIONS AND DISCUSSION

In this paper, we conducted lightning assimilation and precipitation prediction experiments using event data observed by the LMI on board China's FY-4A meteorological satellite. A transformation relationship was established between the lightning frequency and radar reflectivity, and the transformed reflectivity and composite reflectivity of ground-based radar observations exhibited very good consistency. We further assimilated the FY-4 lightning data into the model and adjusted the cloud analysis process so that the model was more objective for hydrometeors of the cloud water, cloud ice and rainwater contents at the initial stage. We adopted a rainstorm event that occurred in central and southern China on August 8, 2017, for the numerical forecast experiment; the corresponding analysis showed that the assimilation of lightning data effectively improved the model's predicted outcome of the extent and intensity of precipitation.

Eastern China hosts a dense ground-based radar observation network. Nevertheless, the overlap between the proxy radar reflectivity obtained via lightning inversion and ground-based radar data limits the efficient application of lightning data. This study demonstrated that the assimilation of lightning data can achieve similar or superior results with respect to the assimilation of the radar reflectivity (Zhang and Zhang [21]). The results of this study provide theoretical support for the operational application of lightning data in areas where radar data cannot be acquired, such as mountains and oceans. Furthermore, the discharge time of convective clouds has been shown to be approximately one hour earlier than the appearance time of radar echoes. As a result, the millisecond-interval data of a lightning detector carried by a geostationary satellite can detect the precursor signal of strong convective weather. Therefore, the assimilation of lightning data in this period excellently complements radar data and has great application potential.

At present, studies on satellite data assimilation that adopt new-generation geostationary satellite LMI data can obtain observations with a high spatiotemporal resolution. Moreover, minute-level and even second-level observations of lightning data can be obtained, and the application potential for weather analysis and weather forecasting is considerable. Therefore, the application of Chinese geostationary meteorological satellite data in forecast models has important research value. Although the findings in this paper are limited to the analyzed case, in the future, we will conduct further evaluations through batch experiments.

REFERENCES:

[1] LIU Rui-xia, XIE Yuan-fu, LIU Jie, et al. A preliminary study on the 3DVAR assimilation of the AMSU-A data in space-time multiscale analysis system [J]. J Trop Meteor, 2017, 23(3): 314-322.

[2] ZHAO Hong, LIU Yin. Experimental application of a thinning scheme for the assimilation of surface observation data in GRAPES-3DVAR [J]. J Trop Meteor, 2018, 24(3): 334-345.

[3] LIU Dong-xia, QIE Xiu-shu, FENG Gui-li. Evolution of lightning characteristic and dynamical structure in a mesoscale convective system over North China [J]. Chin J Atmos Sci, 2010, 34(1): 95-104.

[4] CHANG D E, WEINMAN J A, MORALES C A, et al. The effect of spaceborne microwave and ground-based continuous lighting measurements on forecasts of the 1998 Groundhog- day storm [J]. Mon Wea Rev, 2001, 129(8): 1809-1833.

[5] PESSI A T, BUSINGER S. The impact of lightning data assimilation on a winter storm simulation over the North Pacific Ocean [J]. Mon Wea Rev, 2009, 137 (10): 3177-3195.

[6] WANG Yan-dong, ZHOU Yun-jun, WANG Xi-yang, et al. A study on the assimilation method of lightning data with mesoscale model WRF [J]. J Trop Meteor, 2014, 30(2): 281-292.

[7] BENJAMIN S. Assimilation of lightning data into RUC model convection forecasting, paper presented at Second Conference on Meteorological Applications of Lightning Data [R]. Second Conference on Meteorological Applications of Lightning Data, 2006, Tucson, AZ, 4.3 https://ams.confex.com/ams/Annual2006/techprogram/paper_105079.htm).

[8] FIERRO A O, MANSELL E R, ZIEGLER C L, et al. Application of a lightning data assimilation technique in the WRF-ARW model at cloud-resolving scales for the tornado outbreak of 24 May 2011 [J]. Mon Wea Rev, 2012, 140(8): 2609-2627.

[9] QIE X, ZHU R, YUAN T, et al. Application of total-lightning data assimilation in a mesoscale convective system based on the WRF model [J]. Atmos Res, 2014, 145-146: 255-266.

[10] MARCHAND M R, FUELBERG H E. Assimilation of lightning data using a nudging method involving low-level warming [J]. Mon Wea Rev, 2014, 142(12): 4850-4871.

[11] STEFANESCU R, NAVON I M, FUELBERG H, MARCHAND M. 1D+4D-VAR data assimilation of lightning with WRFDA system using nonlinear observation operators [J]. Physics, 2013.

[12] MANSELL E R. Storm-scale ensemble Kalman filter assimilation of total lightning flash-extent data [J]. Mon Wea Rev, 2014, 142(10): 3683-3695.

[13] LIANG Hua, BAO Shu-long, CHENG Qiang, et al. Design and Implementation of FY-4 Geostationary Lightning Imager [J]. Aerospace Shanghai, 2017, 34(4): 43-51 (in Chinese).

[14] CHRISTIAN H J, BLAKESLEC R J, BOCCIPPIOD J, et al. Global Frequency and distribution of lightning as observed from space by the optical transient detector[J]. J Geophys Res, 2003, 108 (D1), doi: 10.1029/2002JD002347.

[15] FINKE U. Characterising the lightning source for the MTG lightning imager mission [R]. Hannover: Institure für Meteotologie und Klimatologie, 2006.

[16] BAO Shu-long, TANG Shao-fan, LI Yun-fei, et al. Real-time detection technology of instantaneous point-source multi-target lighting signal on geostationary orbit [J]. Infrared and Laser Engineering, 2012, 41(9): 2390-2395.

[17] HUI Wen, HUANG Fu-xiang, GUO Qiang. Application of Hadoop in data-intensive processing of meteorological data[J]. Meteor Sci Technol, 2015, 43(5): 805-813 (in Chinese).

[18] PESSI A. Characteristics of Lightning and Radar Reflectivity in Continental and Oceanic Thunderstorms [C]// 93th Annual American Meteorological Society Meeting, American Meteorological Society, 2013.

[19] PESSI A, ALBERS S. A Lightning Data Assimilation Method for the Local Analysis and Prediction System (LAPS): Impact on Modeling Extreme Events [C]// 94th Annual American Meteorological Society Meeting, American Meteorological Society, 2014.

[20] SAID R K, INAN U S, CUMMINS K L. Long-range lightning geolocation using a VLF radio atmospheric waveform bank [J]. J Geophys Res, 2010, 115, D23108, doi: 101029/2010JD013863.

[21] ZHANG Rong. Assimilation of Lightning Data in Mesoscale Numerical Model [D]. Beijing: Chinese Academy of Meteorological Sciences, 2017: 6 (in Chinese).

Citation: LIU Rui-xia, LIU Jie, PESSI Antti, et al. Preliminary study on the influence of FY-4 lightning data assimilation on precipitation predictions [J]. J Trop Meteor, 2019, 25(4): 528-541.